ISSN 1063-7834, Physics of the Solid State, 2013, Vol. 55, No. 4, pp. 821–828. © Pleiades Publishing, Ltd., 2013.
Original Russian Text © V.S. Bondarev, A.V. Kartashev, M.V. Gorev, I.N. Flerov, E.I. Pogorel'tsev, M.S. Molokeev, S.I. Raevskaya, D.V. Suzdalev, I.P. Raevskii, 2013, published in Fizika Tverdogo Tela, 2013, Vol. 55, No. 4, pp. 752–758.

LATTICE DYNAMICS

Thermal and Physical Properties of Sodium Niobate Ceramics over a Wide Temperature Range

V. S. Bondarev[a, b, *], A. V. Kartashev[a, b], M. V. Gorev[a, b], I. N. Flerov[a, b], E. I. Pogorel'tsev[a, b], M. S. Molokeev[a], S. I. Raevskaya[c], D. V. Suzdalev[c], and I. P. Raevskii[c]

[a] *Kirensky Institute of Physics, Siberian Branch of the Russian Academy of Sciences, Akademgorodok 50–38, Krasnoyarsk, 660036 Russia*

[b] *Institute of Engineering Physics and Radio Electronics, Siberian Federal University, ul. Kirenskogo 28, Krasnoyarsk, 660074 Russia*

* *e-mail: vbondarev@yandex.ru*

[c] *Research Institute of Physics, Southern Federal University, pr. Stachki 194, Rostov-on-Don, 344090 Russia*

Received October 8, 2012

Abstract—The temperature dependences of the heat capacity $C_p(T)$ and thermal expansion coefficient $\alpha(T)$ of $NaNbO_3$ ceramic samples have been investigated in the temperature range from 2 to 800 K. In addition to the anomalies associated with the known phase transitions at temperatures $T_6 \approx 265$ K, $T_5 \approx 638$ K, $T_4 \approx 760$ K, and $T_3 \approx 793$ K, anomalies in the behavior of $C_p(T)$ and $\alpha(T)$ have been observed near $T_{5''} \approx 500$ K and $T_{5'} \approx 600$ K. It has been found that all the observed structural transformations, according to the values of the entropy change, are not related to the ordering of structural elements. It has been shown that, with an increase in the temperature, the unit cell volume during the phase transitions near 265, 515, 604, and 638 K decreases. The specific features of the transition to the phase $R3c$ have been examined. Two possible scenarios of the sequence of phase transformations in the temperature range between T_5 and T_6 have been analyzed.

DOI: 10.1134/S1063783413040045

1. INTRODUCTION

One of the trends in modern materials science is associated with the search for possible ways of replacing lead-containing materials that have been widely used in various technological devices by more environmentally tolerant analogues. A class of promising lead-free functional materials is formed by multicomponent solid solutions based on sodium niobate $NaNbO_3$, which exhibit piezoelectric, pyroelectric, electro-optical, and relaxor properties [1–5]. However, because of the very complex picture of the phenomena observed in $NaNbO_3$ and the related solid solutions, their theoretical description is complicated, and the development of new materials has so far been performed by trial and error.

The difficulties encountered in studying $NaNbO_3$ are associated with the fact that, among the perovskites, this compound undergoes the greatest number of phase transitions of different nature due to rotations of oxygen octahedra and displacement of the ions [6–10]. At present, there is no clear opinion not only about mechanisms of structural distortions but also about the number of phase transformations even in single-crystal $NaNbO_3$. According to [9], we can more or less reliably speak about the existence of the following six structural transformations in $NaNbO_3$:

$$R3c \;(N) \xleftrightarrow{T_6 \approx 250\ \mathrm{K}} Pbcm \;(P) \xleftrightarrow{T_5 \approx 635\ \mathrm{K}} Rmnm \;(R) \xleftrightarrow{T_4 \approx 755\ \mathrm{K}} Pnmm \;(S)$$

$$\xleftrightarrow{T_3 \approx 795\ \mathrm{K}} Ccmm \;(T1) \xleftrightarrow{T_2 \approx 845\ \mathrm{K}} P4/mbm \;(T2) \xleftrightarrow{T_1 \approx 915\ \mathrm{K}} Pm3m. \;(U)$$

The presence of several competing instabilities in $NaNbO_3$ makes this compound very sensitive to external influences and leads, in particular, to the possible coexistence of several phases over a wide temperature range [11–15]. On the one hand, this property can be promising for applications, but, on the other hand, it determines a strong dependence of the properties of $NaNbO_3$-based materials on the preparation conditions, concentration of impurities, and thermal prehistory.

An important basic problem is to derive additional information about phase transitions, specific features of the crystal structure, and physical properties of $NaNbO_3$ with the aim of further developing the model concepts regarding the correlation of phenomena of different physical nature. The solution of this problem will encourage the development of technologies for

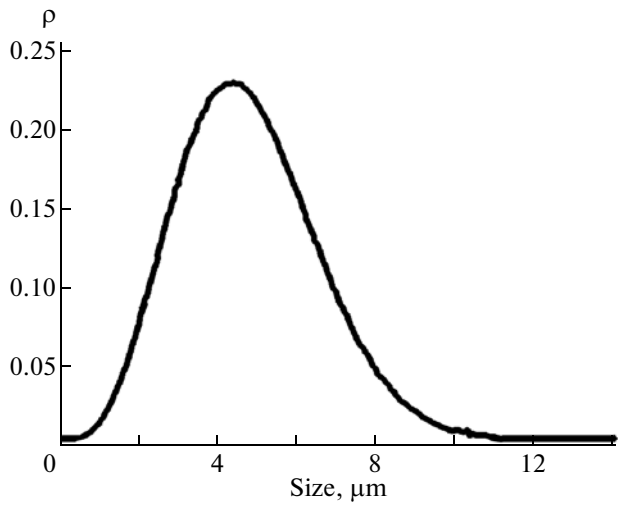

Fig. 1. Grain size distribution in the $NaNbO_3$ ceramic sample according to the X-ray diffraction data.

producing materials with specified and promptly controlled properties.

Although there is a huge amount of studies devoted to $NaNbO_3$ and the related solid solutions, a detailed investigation of their thermal and physical properties has so far not been performed over a wide temperature range, embracing the majority of the known phase transitions. The influence of thermal prehistory of samples of these compounds on the stability of the distorted phases also has not yet been adequately investigated. Thermal and physical properties (heat capacity, thermal expansion) are very sensitive to energy variations in the sample, regardless of their nature, and the relevant investigations can reliably reveal the associated phase transitions. Since $NaNbO_3$-based ceramics have found extensive application in various fields, it is of particular interest to elucidate the nature and mechanism of the phenomena occurring in this type of materials. In this respect, we have carried out investigations of the heat capacity, thermal expansion, and dielectric properties of the $NaNbO_3$ ceramic samples over a wide temperature range (2–800 K).

2. SAMPLES AND EXPERIMENTAL TECHNIQUE

Ceramic samples of sodium niobate $NaNbO_3$ with a density of 92–95% of the theoretical value were prepared by the conventional ceramic technology (solid-phase synthesis with the subsequent calcination at 1200–1220°C without pressure) [2, 10]. All the samples studied by different methods in this work were cut from the same ceramic pellet.

The X-ray diffraction data used for the subsequent refinement of the structure by the Rietveld method were obtained at room temperature on a D8-ADVANCE diffractometer (CuK_α radiation, θ–2θ scan mode) equipped with a VANTEC linear detector. The scan step in the 2θ angle range was 0.016°, and the exposure time per step was 0.3 s. The unit cell parameters were determined with the McMaille4 program [16] and refined during the fitting of the profiles with the DDM program [17]. These investigations revealed that, at room temperature, the $NaNbO_3$ ceramic sample has an orthorhombic symmetry (space group *Pbcm*) with the unit cell parameters $a = 5.50580(4)$ Å, $b = 5.57038(4)$ Å, and $c = 15.52060(8)$ Å, which are in satisfactory agreement with the results reported in [14, 18]. No reflections corresponding to foreign phases on the diffraction patterns were found.

The examination of cleavages of the $NaNbO_3$ ceramic sample with an S-5500 high-resolution scanning electron microscope (Hitachi, Japan) showed that the average grain size was ~4000–5000 nm. However, the sample contained both larger and smaller grains, including those with sizes of ~1000 nm or smaller. The grain size distribution in the $NaNbO_3$ ceramic sample was determined from the X-ray diffraction investigations and corresponded to the electron microscopy data (Fig. 1).

The heat capacity was investigated by several calorimetric methods.

The temperature dependence of the heat capacity $C_p(T)$ was measured on a DSM-10Ma differential scanning microcalorimeter (DSM) at temperatures in the range from 100 to 830 K. The experiments were performed in a helium atmosphere on a sample with a weight of 200 mg in the dynamic mode at rates of change in temperature $dT/d\tau = 8$–16 K min^{-1}. The scatter of the experimental points around the smoothed curve $C_p(T)$ did not exceed 1%. The error in the determination of the integral characteristics (enthalpy and entropy) was equal to ~10–20% depending on the value of the thermal effect.

At temperatures in the range from 2 to 120 K, the temperature dependence of the heat capacity $C_p(T)$ of the sample with a weight of 8 mg was measured using the relaxation method on a Quantum Design PPMS calorimeter. A good thermal contact between the sample and the measurement system was ensured using the Apiezon N low-temperature vacuum grease with a weight of 0.35 mg, whose heat capacity was determined in a separate experiment. The error in the measurement of the heat capacity was less than or equal to 1% below 50 K and approximately equal to 0.25–0.50% above 100 K. The heat capacity measurements in the temperature range from 85 to 300 K were carried out on an adiabatic calorimeter during heating in the discrete mode ($T = 1.8$–2.5 K) and in the continuous mode ($dT/d\tau = 0.18$–0.22 K min^{-1}). Methodological features of the heat capacity measurements were described in more details in [19].

The thermal expansion of the sample with a length of 4.74 mm was investigated in the temperature range 90–770 K on a NETZSCH DIL-402C dilatometer in the dynamic mode during heating and cooling at rates $dT/d\tau = 2$–5 K min^{-1}. The measurements were performed in a helium stream. For the calibration and correction for the thermal expansion of the measurement system, we used reference samples of fused silica and corundum.

The dielectric permittivity was measured in the temperature range 100–300 K on an E7-20 immittance meter in the heating and cooling modes at a rate of ~0.6 K min^{-1}. The measurements were carried out on a sample 10 mm in diameter and 2 mm in height with electrodes made of silver leaf.

3. EXPERIMENTAL RESULTS

The performed investigations of the thermal and physical properties revealed seven anomalies of the heat capacity (Fig. 2); however, only six of these anomalies were reproduced from series to series of measurements, or, more precisely, the anomalies observed at temperatures of 262, 515, 604, 638, 760, and 793 K. A comparison of these data with the scheme given in the Introduction demonstrates that only two peaks, namely, at the peak at $T_{5''} = 515$ K and the peak at $T_{5'} = 604$ K, do not correspond to the known phase transitions observed in $NaNbO_3$ [9].

In what follows, we will be interested only in the anomalous heat capacity, which is defined as the difference between the total heat capacity and the lattice components: $\Delta C_p = C_p - C_L$. The latter quantity was obtained by fitting the data on the dependence $C_p(T)$ with a polynomial function outside the region of the anomalous behavior.

The anomaly ΔC_p revealed at ~720 K in a series of measurements presented in Fig. 2 was influenced by thermal cycling, which was reflected in a significant change in both the amplitude of this anomaly and its position on the temperature scale. That is why we do not tend to associate this anomaly with a phase transition in $NaNbO_3$, as was assumed in [7].

The measurements carried out in the cooling mode revealed only three anomalies of the heat capacity at temperatures $T_{5'} \approx 530$ K, $T_5 \approx 578$ K, and $T_3 \approx 775$ K; i.e., the corresponding temperature hystereses were ~75, ~60, and ~18 K, respectively.

The integration of the function $(\Delta C_p/T)(T)$ over the entire temperature range under investigation made it possible to determine the total change in the entropy $\Delta S = 4.0$ J (mol K)$^{-1}$ due to the revealed sequence of phase transitions (see inset in Fig. 2). The calculation of the entropy ΔS_i for each of the transformations at the aforementioned temperatures T_i is rather complicated, because the heat capacity anomalies either are diffuse or are overlapped. We can make only rough

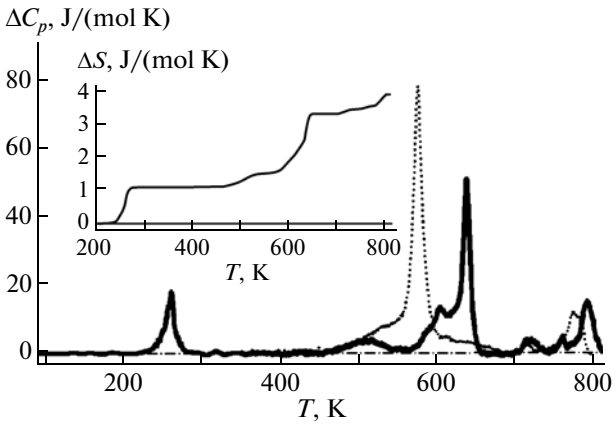

Fig. 2. Temperature dependences of the excess heat capacity ΔC_p and the excess entropy ΔS (inset) measured in the heating mode (solid line) and in the cooling mode (dotted line).

estimates: $\Delta S_6 \approx 1.2$ J (mol K)$^{-1}$, $\Delta S_{5''} \approx 1.0$ J (mol K)$^{-1}$, $\Delta S_{5'} \approx 0.5$ J (mol K)$^{-1}$, $\Delta S_5 \approx 0.8$ J (mol K)$^{-1}$, $\Delta S_4 \approx 0.1$ J (mol K)$^{-1}$, and $\Delta S_3 \approx 0.5$ J (mol K)$^{-1}$. Some of our values ΔS_i considerably exceed the entropy changes determined in [20, 21], but, nonetheless, remain to be characteristic of displacive phase transformations.

As was noted in the Introduction, the $NaNbO_3$ niobate is very sensitive to various factors. This property is most pronounced in the case of the phase transition at the temperature T_6, which, in the $NaNbO_3$ single crystal, is characterized by a significant hysteresis, but was observed not in all studies [6, 22]. In calorimetric measurements on the differential scanning microcalorimeter, we reliably revealed an anomaly of the heat capacity in the ceramic sample at 262 K in the heating mode. In order to refine the thermodynamic parameters of the phase transitions, we performed more detailed investigations of the heat capacity at low temperatures on the adiabatic calorimeter and the PPMS calorimeter. The results of these measurements are presented in Fig. 3. It can be seen that the data on the dependence $C_p(T)$ measured using the adiabatic calorimeter and the PPMS calorimeter are in satisfactory agreement in the range of their overlapping (85–120 K).

The temperature dependence of the heat capacity measured on the adiabatic calorimeter during heating of the sample after cooling to 78 K exhibits an anomaly at $T_6 = 265$ K (Fig. 3). Taking into account that the phase transition $R3c \longrightarrow Pbcm$ is characterized by an anomalously large hysteresis [6, 22], we also measured the dependence $C_p(T)$ after cooling of the sample to 200 K. It can be seen from Fig. 3 (lower inset) that, in this case, there is no anomaly of the heat capacity.

In order to separate the lattice (C_L) and anomalous (ΔC_p) contributions to the heat capacity, we used a

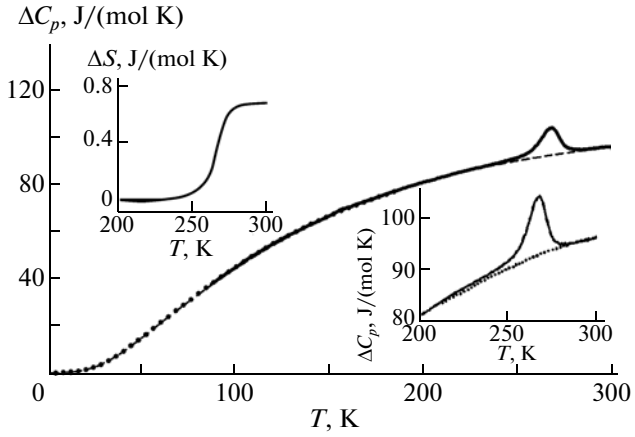

Fig. 3. Temperature dependence of the heat capacity of the $NaNbO_3$ ceramic sample measured during heating from 85 K (solid line). The dashed line shows the dependence of the lattice heat capacity $C_L(T)$ calculated using a combination of the Debye and Einstein functions. Points represent the dependence $C_p(T)$ measured on the PPMS calorimeter. The lower inset shows the dependence $C_p(T)$ measured in the heating mode after cooling to 85 K (solid line) and 200 K (dotted line). The upper inset shows the behavior of the excess entropy.

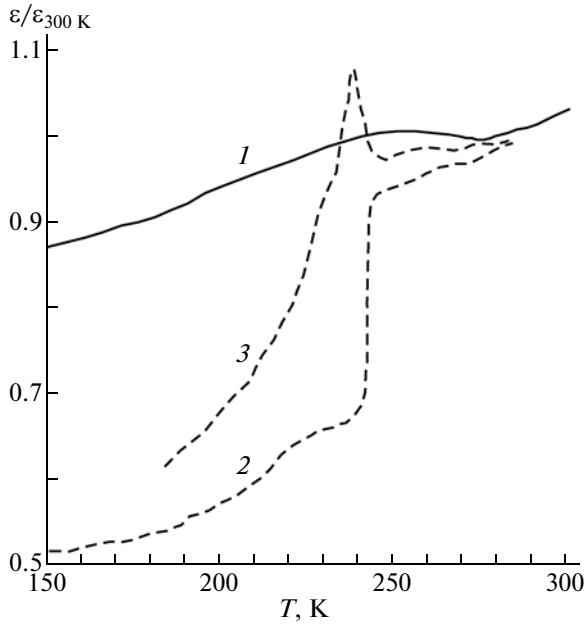

Fig. 4. Dependences $\varepsilon(T)$ measured in the heating mode and normalized to the value of ε at 300 K: (*1*) $NaNbO_3$ ceramic sample, (*2*) $NaNbO_3$ single crystal containing only the antiferroelectric phase *P* at room temperature, and (*3*) oxygen-deficient $NaNbO_3$ single crystal containing approximately 50% of the ferroelectric phase *Q* at room temperature.

simple model describing the dependence $C_L(T)$ by a combination of the Debye and Einstein functions (dashed line in Fig. 3):

$$C_p(T) = C_{V(D)}(\Theta_D, T) + C_{V(E)}(\Theta_E, T).$$

Here, the difference between the heat capacities C_p and C_V was ignored, because, in this case, its value is relatively small due to the smallness of the thermal expansion coefficients of the $NaNbO_3$ compound. The Debye and Einstein temperatures involved in the above equation were found to be $\Theta_E = 560$ K and $\Theta_D = 310$ K, respectively. The behavior of the calculated dependence $C_L(T)$ coincides with the behavior of the dependence $C_p(T)$ obtained in measurements from 200 K (dotted line in the lower inset to Fig. 3). Therefore, in the latter case, the sample is in the phase *Pbcm*. This feature will be considered in more details when analyzing the data obtained in the investigation of the thermal expansion.

The change in the entropy ΔS_6 was found to be ~0.7 J (mol K)$^{-1}$ (upper inset to Fig. 3); as a result, the phase transition $R3c \longrightarrow Pbcm$ can be characterized as the displacive phase transition. A close value of the entropy change (0.82 J (mol K)$^{-1}$) in the low-temperature phase transition was also obtained in the $Li_{0.02}Na_{0.98}NbO_3$ crystal [23], where the phase transition was observed at 260 K in the heating mode.

The results obtained from measurements of the permittivity ε of the $NaNbO_3$ ceramic sample at a frequency of 1 MHz are presented in Fig. 4. It can be seen from this figure that, in the heating mode at temperatures in the range from 230 to 270 K, the dependence $\varepsilon(T)$ exhibits a diffuse anomaly (curve *1*). The shape of this anomaly differs from that observed in the dependence $\varepsilon(T)$ of the $NaNbO_3$ single crystal due to the phase transition $R3c \longrightarrow Pbcm$ (curve *2*), but it is qualitatively similar to the anomaly revealed in the dependence $\varepsilon(T)$ of the oxygen-deficient $NaNbO_3$ single crystal, which, according to the X-ray powder diffraction data, contains at room temperature approximately 50% of the ferroelectric phase *Q* (curve *3*) [14, 22]. During the cooling to liquid-nitrogen temperature, no specific features in the dependence $\varepsilon(T)$ of the $NaNbO_3$ ceramic sample was found.

Figure 5a presents the results obtained from the investigation of the thermal expansion of the $NaNbO_3$ ceramic sample in four consecutive series of measurements. In all cases, the temperature dependence of the thermal expansion coefficient α exhibits three clearly pronounced anomalies at temperatures $T_6 = 270 \pm 1$ K, $T_{5''} \approx 530$ K, and $T_5 = 640 \pm 1$ K and a small anomaly at $T_{5'} \approx 604$ K. A small difference between the temperatures of anomalies in the dependences $C_p(T)$ and $\alpha(T)$ is associated with the different conditions of measurements in the calorimeter and in the dilatometer. The thermal expansion measurements in the heating and cooling modes revealed a temperature hysteresis $\delta T_5 \approx 55$ K due to the phase transition $Pbcm \longrightarrow Pmnm$ (see inset in Fig. 5).

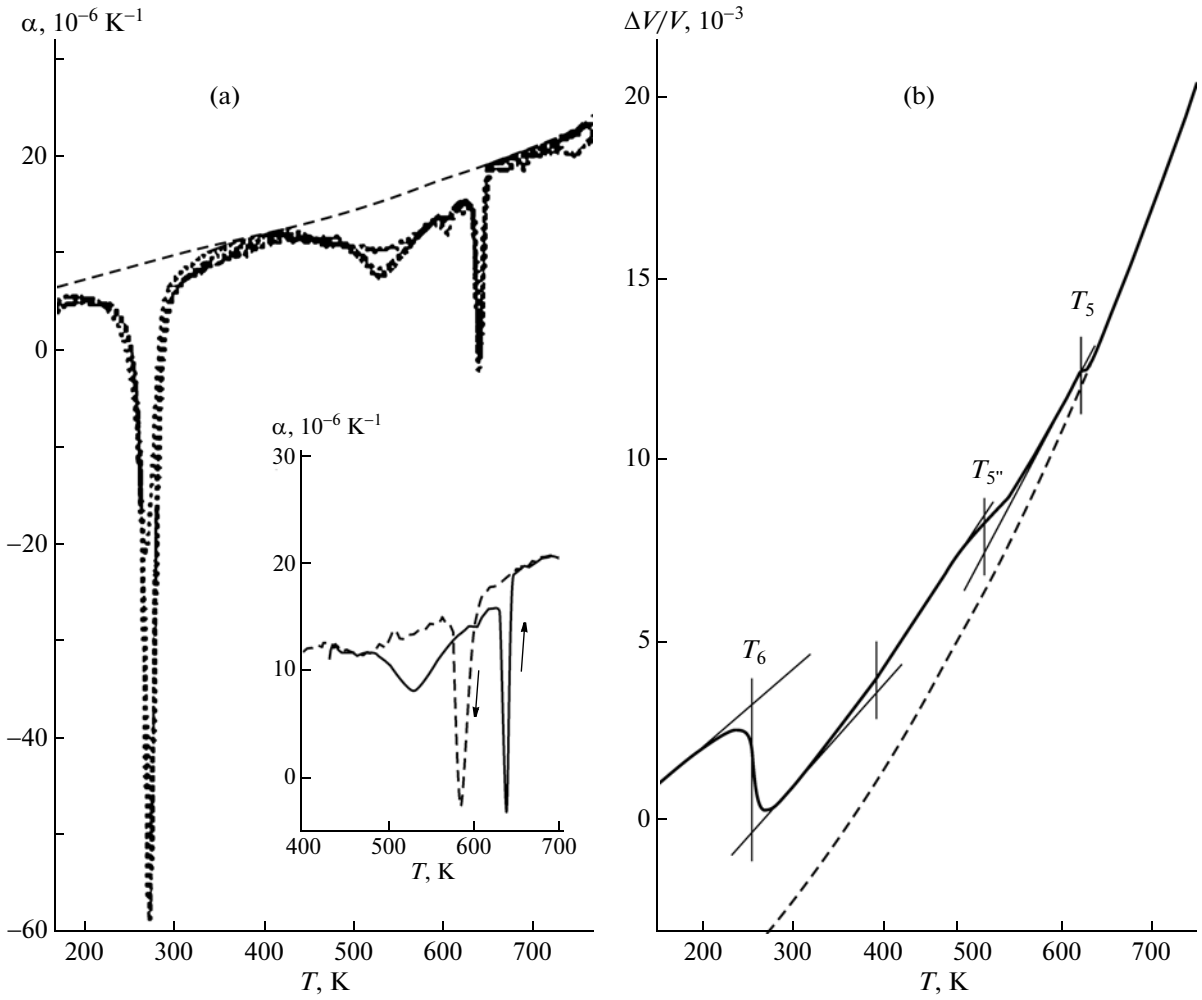

Fig. 5. (a) Temperature dependences of the thermal expansion coefficient α of the $NaNbO_3$ ceramic sample in four consecutive series of measurements (dotted lines). The dashed line shows the lattice component. The inset shows the dependence $\alpha(T)$ measured in the heating and cooling modes. (b) Volume deformation $\Delta V/V$ (see text).

The most significant difference is observed only for the results obtained in the first series of measurements (Fig. 5a). In all the subsequent experiments, after heating of the sample to 770 K (in the first series), the anomalies at 270 and 530 K increase significantly, whereas the anomaly at 604 K decreases. The behavior of the dependence $\alpha(T)$ in the region of the anomaly at 640 K remains almost unchanged. Moreover, at temperatures above ~650 K, the thermal expansion coefficient increases. This behavior of the thermal expansion coefficient can be associated with the annealing of defects and stresses during heating in the first series of measurements, as well as with the change in the composition of the sample after exposure to an oxygen-free atmosphere at high temperatures. However, annealing in a helium atmosphere for one hour at temperatures of 590, 603, 615, and 750 K did not lead to a significant change in the behavior of the thermal expansion over the entire temperature range under investigation. This indicates that the possible changes in the composition of the sample after exposure to an oxygen-free atmosphere at temperatures used in the experiments do not affect the obtained results.

Taking into account the specific features in the behavior of the heat capacity of the $NaNbO_3$ sample at the temperature T_6, we carried out experiments on the influence of the cooling depth of the sample and the time of its holding at $T < T_6$ on the corresponding anomaly of the thermal expansion coefficient. It can be seen from Fig. 6 that the variation of the two factors leads to a significant change in the anomaly of the thermal expansion coefficient. During cooling of the sample to $T \geq 200$ K, an anomaly of the thermal expansion was not observed at all, which is consistent with the corresponding results obtained from the investigation of the heat capacity.

The dashed line in Fig. 5 shows the behavior of non-anomalous (lattice) components of the thermal expansion coefficient α_L and the deformation

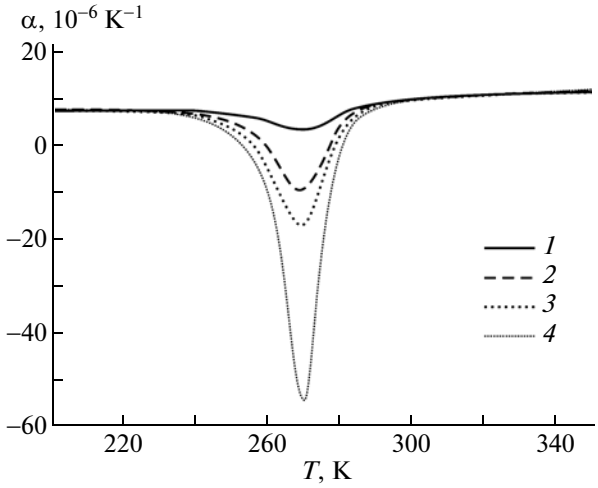

Fig. 6. Temperature dependences of the thermal expansion coefficient of the $NaNbO_3$ sample measured at low temperatures in the heating mode after holding at temperatures $T = (1)$ 170, (*3*) 120, and (*4*) 90 K for 10 min and (*2*) after holding at $T = 170$ K for 60 min.

$(\Delta L/L)_L$. For their determination, we used the expression $C_L(T) = K\alpha_L(T)$ relating the thermal expansion coefficient and the heat capacity. The lattice heat capacity was determined according to the equation which we obtained in the processing of the low-temperature heat capacity data. In order to take into account the additional contributions due to the difference in the heat capacities C_p and C_V at high temperatures, as well as the possible contributions to the thermal expansion due to the formation of vacancies and other defects, we introduced two additional terms into the equation, i.e., $A_1T + A_2T^2$. The coefficients K, A_1, and A_2 were determined from the values of the thermal expansion coefficients obtained at $T > 670$ K. The deformation in the temperature range 120–770 K is shown in Fig. 5b.

4. DISCUSSION

We consider the obtained results with respect to the changes in the structure of the $NaNbO_3$ sample at specific temperatures.

The anomalous behavior of the heat capacity of the $NaNbO_3$ sample at the temperatures $T_3 = 793$ K and $T_4 = 760$ K is obviously associated with the successive rotational phase transitions $Ccmm(T_1) \longrightarrow Pnmm(S) \longrightarrow Pmnm(R)$ [9]. In the dilatometric experiments, the region of these temperatures was inaccessible.

The anomalous behavior of the thermal expansion and heat capacity of the $NaNbO_3$ sample at $T_5 \approx 640$ K is associated with the changes in the structure due to the known phase transition to the antiferroelectric phase $Pmnm(R) \longrightarrow Pbcm(P)$ [9].

According to [9], at temperatures $T < T_5$, no structural changes in the ideal defect-free crystal of the $NaNbO_3$ compound occur down to T_6, which corresponds to the temperature of the transition to the ferroelectric phase $R3c(N)$. However, in our samples, we observed clearly pronounced and well-reproduced anomalies of $C_p(T)$ and $\alpha(T)$ at the temperatures $T_{5'}$ and $T_{5''}$.

In the papers devoted to the analysis of the phase transitions in $NaNbO_3$, it is noted that, at room temperature, the antiferroelectric phase $Pbcm(P)$ and the ferroelectric $Pmc2_1(Q)$ phase, whose energies are very close to each other, can coexist in the sample. In the case when the Q phase exists at a lower temperature than the phase transition $R \longrightarrow P$, the phase transition $P \longrightarrow Q$ is observed in the sample [14, 15, 24]. The coexistence of the phases P and Q at room temperature in crystals and ceramic samples of $NaNbO_3$ was repeatedly noted in a number of experimental works [11, 14, 15, 25]. The observed anomalies in the physical properties at temperatures in the range between T_6 and T_5 are explained precisely by the presence of the Q phase in the sample [15, 21]. As a rule, the formation of the Q phase is explained by the fact that the samples contain defects or heterogeneities that are favorable to its stabilization [13, 15].

Detailed investigations of the structure and Raman spectra of $NaNbO_3$ powders revealed that, in particles of different sizes d at room temperature, there can exist different phases: $Pbcm(P)$ ($d \geq 1100$ nm), $Pmc2_1(Q)$ ($d = 200$–600 nm), and $Pbma$ ($d \leq 120$ nm) [21]. It was also shown that the transitions to these phases from the phase $Pmnm(R)$ occur at temperatures of 635, ~580–600, and ~450–500 K, respectively.

The anomalous behavior of the thermal expansion and heat capacity in the range of temperatures $T_{5'}$ and $T_{5''}$, which was revealed in our work (Figs. 2 and 5), most likely, is also a consequence of the structural heterogeneity of crystal grains, which leads to differences in their physical properties, and is associated with the hypothetical phase transitions between the phases P, Q, and R. The factors responsible for the appearance of the structural heterogeneity in samples cannot be determined only on the basis of the performed investigations. The solution of this problem requires additional thorough investigations of the structure in this temperature range. We can only assume several possible scenarios of the phenomena occurring in this case on the basis of the data available in the literature.

The analysis carried out in the framework of the thermodynamic approach [24] leads to the conclusion that the free energies of the phases P and Q in $NaNbO_3$ intersect at two temperatures, and the Q phase is stable in the temperature range 393–533 K. However, in the oxygen-deficient $NaNbO_3$ single crystals, the Q phase was observed at considerably lower temperatures [14, 15]. In the presence of heterogeneities in the sample,

some of the regions undergo a phase transition from the P phase to the Q phase near 429 K. From the structural point of view, this is associated with the disappearance of anti-phase rotations of the octahedra around the orthorhombic b axis and the change in the ordering of Nb cations from antiferroelectric to ferroelectric. According to [26], the Q phase is stable in a limited temperature range; at 588 K, it transforms into another phase, probably, similar to the P phase, which then transforms into the R phase.

Taking into account the results of the structural and dielectric studies [11, 13–15, 25, 27], in which it was established that, at room temperature, only the phases P and Q coexist, as well as the agreement of the temperature $T_{5''}$ with the temperature of the loss of pyroelectric activity [27] and a large jump in the volume at this temperature [21], we can assume that it is at this temperature $T_{5''}$ that there occurs a transition from the polar phase Q to a nonpolar phase. Although we did not reveal noticeable anomalies in the behavior of $C_p(T)$ and $\alpha(T)$ due to the expected phase transition $P \longrightarrow Q$ in the temperature range 350–450 K, it is in this range that the temperature dependence of the volume deformation exhibits a kink (Fig. 5b).

A comparison of the volume changes ΔV obtained in [21] due to the phase transition $Pbcm(P) \longrightarrow Pmnm(R)$ for the case $d > 1100$ nm and the phase transition $Pmc2_1(Q) \longrightarrow Pmnm(R)$ for $d \sim 280$ nm with the values of ΔV determined at the temperatures T_5 and $T_{5''}$ in our work (Fig. 5b) allows us to estimate the content of the phases $Pbcm(P)$ (70–80%) and $Pmc2_1(Q)$ (20–30%) in the studied sample. This phase relationship is in satisfactory agreement with the data of structural studies [14, 25].

It should be noted that, with this interpretation, the nature of the anomalies revealed at $T_{5'}$ in the heat capacity $C_p(T)$ and thermal expansion $\alpha(T)$ of our samples remains unclear.

On the other hand, we can attempt to explain the specific features in the behavior of both the heat capacity and the thermal expansion at the temperatures $T_{5''}$ and $T_{5'}$ in terms of the size effects observed and investigated in [21]. The analysis of the microstructure of the $NaNbO_3$ compound confirms the presence of grains of different sizes in the sample. According to the X-ray diffraction data (Fig. 1), the volume of the $NaNbO_3$ sample is inhomogeneous and include regions with sizes $d = 100$–5000 nm; i.e., it consists of micro- and nanoregions. Taking into account this circumstance and the data reported in [21], it can be assumed that, in the sample at room temperature, there exist two antiferroelectric phases (*Pbcm* and *Pmma*) and one ferroelectric phase ($Pmc2_1(Q)$). During heating, the phase transition $Pmma \longrightarrow Pmnm(R)$ occurs at the temperature $T_{5''}$, whereas the polar phase $Pmc2_1(Q)$ transforms into the phase $Pmnm(R)$ at the temperature $T_{5'}$. At the temperature T_5, the nonpolar phase $Pbcm(P)$ transforms into the phase $Pmnm(R)$. This sequence of phase transformations is in satisfactory agreement with the experimental calorimetric and dilatometric data obtained in our work. In the cooling mode, according to [21], there is a sequence of two phase transitions at the temperatures $T_{5'}$ and T_5, whereas at the temperature $T_{5''}$, no features are found. A similar sequence of phase transitions was also observed in our thermal experiments.

Although the temperatures of phase transitions in micro- and nanoregions are in agreement with the temperatures T_5, $T_{5'}$, and $T_{5''}$ of the anomalies in the dependences $C_p(T)$ and $\alpha(T)$, the large change in the volume at the temperature $T_{5''}$, which was determined from our data on the thermal expansion, is not comparable to the changes in the volume during the phase transition $Pmma \longrightarrow Pmnm(R)$ [21].

The anomalies of $C_p(T)$ and $\alpha(T)$ at the temperature T_6 are related to the phase transition from the ferroelectric phase $R3c(N)$ to the antiferroelectric phase P. The temperature of this transition, as determined in different works in the heating and/or cooling modes, varies over a wide range (~50–300 K) and is characterized by a very large hysteresis $\delta T \geq 100$ K [6, 22]. Both of these factors indicate that the equilibrium temperature of the phases $Pbcm(P)$ and $R3c(N)$ can be significantly influenced by defects and heterogeneities of the crystal structure or by external effects.

The temperature dependence of the volume change $\Delta V(T)$ indicates that, with a decrease in the temperature, the lattice volume increases as a result of the phase transitions at temperatures T_5, $T_{5'}$, $T_{5''}$, and T_6. According to the Clausius–Clapeyron equation $dT/dp = \delta V/\delta S$, this means that the corresponding temperatures decrease with an increase in the hydrostatic pressure.

5. CONCLUSIONS

The calorimetric and dilatometric investigations of the $NaNbO_3$ ceramic sample have revealed anomalies in the behavior of the heat capacity and thermal expansion, which correspond to the successive phase transitions $Ccmm(T_1) \longrightarrow Pnmm(S) \longrightarrow Pmnm(R) \longrightarrow Pbcm(P) \longrightarrow R3c(N)$. It has also been found that the thermal and physical properties of $NaNbO_3$ exhibit significant features at temperatures $T_{5'}$ and $T_{5''}$, which are not related to the known phase transitions. Two possible variants of the sequence of phase transformations in the temperature range between T_5 and T_6 have been analyzed under the assumption that, in the ceramic sample, several phases with different symmetries exist at room temperature.

The analysis of the temperature dependence of the entropy has demonstrated that the mechanism of

structural distortions revealed in this work is associated with small atomic displacements.

The kinetic features of the transition to the phase *R*3*c* have been examined. It has been found that the values of the corresponding anomalies of the heat capacity C_p and the thermal expansion coefficient α substantially depend on the depth of cooling the sample prior to measurements in the heating mode and on the time of holding the sample at $T < T_6$.

ACKNOWLEDGMENTS

This study was supported by the Council on Grants from the President of the Russian Federation for Support of Leading Scientific Schools of the Russian Federation (grant no. NSh-4828.2012.2) and the Russian Foundation for Basic Research (project no. 12-02-31799_mol_a).

REFERENCES

1. Y. Saito, H. Takao, T. Tani, T. Nonoyama, K. Takatori, T. Homma, T. Nagaya, and M. Nakamura, Nature (London) **432**, 84 (2004).
2. I. P. Raevski, L. A. Reznitchenko, M. A. Malitskaya, L. A. Shilkina, S. O. Lisitsina, S. I. Raevskaya, and E. M. Kuznetsova, Ferroelectrics **299** (1–2), 95 (2004).
3. S. I. Raevskaya, L. A. Reznichenko, I. P. Raevski, V. V. Titov, and S. V. Titov, Ferroelectrics **340**, 107 (2006).
4. T. R. Shrout and S. J. Zhang, J. Electroceram. **19**, 111 (2007).
5. V. V. Shvartsman and D. C. Lupascu, J. Am. Ceram. Soc. **95** (1), 1 (2012).
6. L. E. Cross and B. J. Nicholson, Philos. Mag. **46** (376), 453 (1955).
7. R. Ishida and G. Honjo, J. Phys. Soc. Jpn. **34** (11), 1279 (1973).
8. K. S. Aleksandrov, A. T. Anistratov, B. V. Beznosikov, and N. V. Fedoseeva, *Phase Transitions in Crystals of ABX_3 Halide Compounds* (Nauka, Novosibirsk, 1981) [in Russian].
9. H. D. Megaw, Ferroelectrics **7** (1–4), 87 (1974).
10. M. P. Ivliev, S. I. Raevskaya, I. P. Raevskii, V. A. Shuvaeva, and I. V. Pirog, Phys. Solid State **49** (4), 769 (2007).
11. I. Lefkowitz, K. Lukaszewicz, and H. D. Megaw, Acta Crystallogr. **20**, 670 (1966).
12. E. A. Wood, R. C. Miller, and J. P. Remeica, Acta Crystallogr. **15**, 1273 (1962).
13. J. Chen and D. Feng, Phys. Status Solidi A **109**, 171 (1988).
14. L. A. Reznichenko, L. A. Shilkina, E. S. Gagarina, I. P. Raevskii, E. A. Dul'kin, E. M. Kuznetsova, and V. V. Akhnazarova, Crystallogr. Rep. **48** (3), 448 (2003).
15. R. A. Shakhovoy, S. I. Raevskaya, L. A. Shakhovaya, D. V. Suzdalev, I. P. Raevski, Yu. I. Yuzyuk, A. F. Semenchev, and M. El Marssi, J. Raman Spectrosc. **43**, 1141 (2012).
16. A. Le Bail, Powder Diffr. **19**, 249 (2004).
17. L. A. Solovyov, J. Appl. Crystallogr. **37**, 1 (2004).
18. A. C. Sakowski-Cowley, K. Lukaszewicz, and H. D. Megaw, Acta Crystallogr., Sect. B: Struct. Crystallogr. Cryst. Chem. **25**, 851 (1969).
19. A. V. Kartashev, I. N. Flerov, N. V. Volkov, and K. A. Sablina, Phys. Solid State **50** (11), 2115 (2008).
20. I. Pozdnyakova, A. Navrotsky, L. Shilkina, and L. Reznitchenko. J. Am. Ceram. Soc. **85** (2), 379 (2002).
21. Y. Shiratori, A. Magrez, W. Fischer, Ch. Pithan, and R. Waser, J. Phys. Chem. C **111**, 18493 (2007).
22. S. I. Raevskaya, I. P. Raevski, S. P. Kubrin, M. S. Panchelyuga, V. G. Smotrakov, V. V. Eremkin, and S. A. Prosandeev, J. Phys.: Condens. Matter **20**, 232202 (2008).
23. W. L. Zhong, P. L. Zhang, H. S. Zhao, Z. H. Yang, Y. Y. Song, and H. C. Chen, Phys. Rev. B: Condens. Matter **47**, 10583 (1992).
24. C. N. W. Darlington, Philos. Mag. **31**, 1159 (1975).
25. K. E. Johnston, C. C. Tang, J. E. Parker, K. S. Knight, P. Lightfoot, and S. E. Ashbrook, J. Am. Chem. Soc. **132**, 8732 (2010).
26. R. Jiménez, M. L. Sanjuán, and B. Jiménez, J. Phys.: Condens. Matter **16**, 7493 (2004).
27. K. Konieczny, Mater. Sci. Eng., B **60**, 124 (1999).

Translated by O. Borovik-Romanova